Microstructure evolution during annealing of an SPD- processed supersaturated Cu – 3 at.% Ag alloy

To cite this article: J Gubicza *et al* 2014 *IOP Conf. Ser.: Mater. Sci. Eng.* **63** 012091

View the article online for updates and enhancements.

Related content

Microstructure evolution during annealing of an SPD-processed supersaturated Cu – 3 at.% Ag alloy

J Gubicza[1], Z Hegedűs[1,2], J L Lábár[1,3], V Subramanya Sarma[4],

A Kauffmann[5,6] and J Freudenberger[5]

[1]Department of Materials Physics, Eötvös Loránd University, Budapest, P.O.B. 32, H-1518, Hungary
[2]Max Planck Institute for Intelligent Systems, Heisenbergstrasse 3, D-70569 Stuttgart, Germany
[3]Research Institute for Technical Physics and Materials Science, Research Centre for Natural Sciences, Hungarian Academy of Sciences, P.O.Box 49, H-1525 Budapest, Hungary
[4]Department of Metallurgical and Materials Engineering, Indian Institute of Technology Madras, Chennai, 600036 India
[5]IFW Dresden, P.O. Box 270116, 01171 Dresden, Germany
[6]TU Dresden, Institute of Materials Science, 01062 Dresden, Germany

Email: jeno.gubicza@ttk.elte.hu

Abstract. Supersaturated Cu – 3 at.% Ag alloy was processed by rolling at liquid nitrogen temperature and subsequent annealing at 623 K up to 20 min. It was found that after annealing, an inhomogeneous solute atom distribution developed, since the Ag particles with small size and/or large specific interfacial energy were dissolved due to the Gibbs-Thomson effect. In the region where the solute concentration increased, a high dislocation density was retained in the Cu matrix even after annealing, while in the region where the Ag solute content did not increase, the dislocation density decreased by more than one order of magnitude. Therefore, in the cryorolled and annealed samples, heterogeneous microstructures were developed where both the dislocation density and the solute concentration varied considerably.

1. Introduction

The mechanical properties of metallic materials can be improved by severe plastic deformation (SPD) techniques [1,2]. The increment in the lattice defect densities (such as dislocations) and the grain refinement during SPD yield enhancement of the strength. The SPD-induced strength increment can be further enhanced by alloying as the additive elements have a pinning effect on dislocations and grain boundaries [3,4]. The alloying element concentration before SPD can be increased even into the supersaturated level applying solution heat treatment and subsequent quenching. However, it was revealed that the increase of the strength in these ultrafine-grained (UFG) materials was accompanied by a reduction of the tensile ductility due to the loss of strain hardening capacity of the samples [5]. Moderate heat-treatments after SPD were successfully applied in order to increase the ductility considerably while retaining the high strength [6,7]. In the annealing step of these thermomechanical treatments usually heterogeneous structural relaxation (i.e. recovery and recrystallization) occurs. In

the relaxed volumes the dislocation density can increase again during tensile test, leading to considerable strain hardening which results in an improved ductility of the material. In pure metals, the heat-treatment often yields bimodal grain structures with coarse recrystallized grains embedded in an UFG matrix. A recent report [8] has shown that a combination of high strength and good ductility can be achieved in supersaturated Cu – 3 at.% Ag alloy by applying a moderate annealing after rolling at liquid nitrogen temperature (LNT). The cryorolled sample exhibited high ultimate tensile strength (UTS) of about 710 MPa with negligible uniform elongation (~ 1%). After annealing for 5 min at 648 K, the UTS decreased only slightly (by ~ 60 MPa) with significant improvement in the uniform elongation (from 1 to 8%). These changes in the mechanical properties were attributed to the formation of an inhomogeneous microstructure. In some volumes, the dislocation density decreased considerably which contributed to the work hardening during subsequent tension, thereby increasing the uniform elongation as compared to the cryorolled specimens. In this paper, a systematic study on the evolution of the microstructure during isothermal annealing of cryorolled Cu – 3 at.% Ag alloy is presented.

2. Experimental

Cu – 3 at.% Ag alloy was prepared by induction melting in Ar atmosphere from high purity (99.9%) elements and casting them into $15 \times 15 \times 150$ mm^3 graphite moulds. The alloy was homogenized at 750 °C (1023 K) for 5 h and subsequently was quenched in water. The homogenized plate was subjected to rolling at LNT (~77 K) to a strain of ~2. Analysis of differential scanning calorimetry measurements at a heating rate of 10 K/min showed that recovery and recrystallization in the LNT rolled sample start at ~623-648 K [8]. In order to investigate the evolution of the microstructure during annealing, cryorolled samples were heat-treated isothermally at 623 K for 5, 10, 15 and 20 min. The effect of this annealing on the microstructure was investigated by X-ray diffraction (XRD). The X-ray diffraction patterns were measured by a high-resolution rotating anode diffractometer (type: RA-MultiMax9, manufacturer: Rigaku) using CuKα_1 (λ=0.15406 nm) radiation. Two-dimensional imaging plates were used to detect the Debye-Scherrer diffraction rings. The line profiles (perpendicular to the rings) were obtained by integrating the two dimensional intensity distribution along the rings. The lattice constant was determined by the Nelson–Riley extrapolation method [9]. The X-ray diffraction line profiles were evaluated for the microstructure by the Convolutional Multiple Whole Profile (CMWP) fitting method [10]. In this procedure, the diffraction pattern is fitted by the sum of a background spline and the convolution of the instrumental pattern and the theoretical line profiles related to the crystallite size, dislocations and twin faults. As an example, the fitting for the LNT rolled specimen is shown in Fig. 1. The theoretical profile functions used in this fitting procedure were calculated on the basis of a model of the microstructure, where the crystallites have spherical shape and log-normal size distribution. The following parameters of the microstructure were obtained from the CMWP fitting procedure: the area weighted mean crystallite size ($<x>_{area}$), the dislocation density (ρ) and the twin boundary probability (β). The twin boundary probability is defined as the fraction of twin faults among the {111} lattice planes.

Complementary transmission electron microscopy (TEM) investigations were carried out on the cryorolled specimen and the samples annealed at 623 K for 10 and 20 min. TEM lamellae were prepared with special care to avoid additional unwanted annealing of the samples. Low temperature glue (GATAN G1) was used at 60°C to fix the sample in the 3 mm diameter Ti disk. Ion milling was carried out at 7 keV with continuous cooling of the sample by liquid nitrogen. TEM examinations were performed in a JEOL 3010 operated at 300 keV. Images and diffraction patterns were recorded with a GATAN Orius camera, designed to withstand diffraction patterns. The diffraction patterns were indexed with the help of the ProcessDiffraction program [11]. Distances in the Moiré pattern were measured with the commercial Digital Micrograph program.
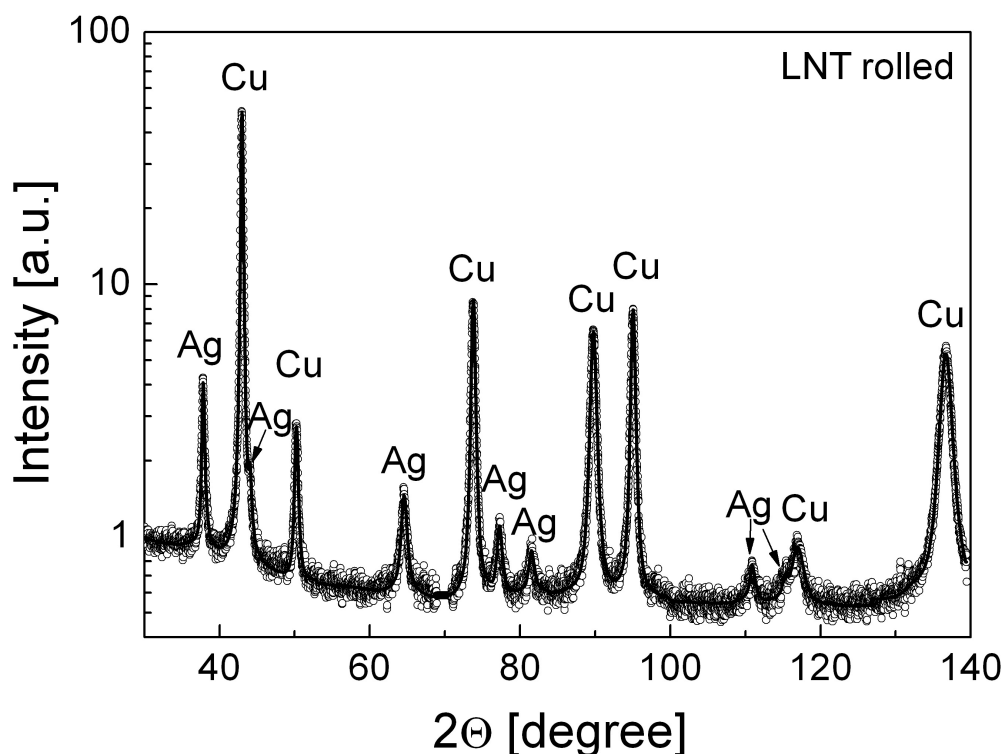
Figure 1. The fitting of the X-ray diffraction pattern for the LNT rolled Cu − 3 at.% Ag by the CMWP method. The open circles and the solid line represent the measured data and the fitted curves, respectively. The intensity is in logarithmic scale.

3. Results

The Ag solute content in the Cu matrix was determined from the lattice parameter measured by XRD and the values are listed in Table 1. According to Ref. [12], the lattice constant for dilute Cu-Ag alloys increases linearly with the Ag concentration and 1 at.% Ag in solution yields an increment of 0.0007 nm in the lattice parameter of Cu (for pure Cu the lattice parameter is 0.3615 nm). The Ag concentration in the Cu matrix of the LNT rolled sample was estimated to be 1.0 ± 0.1 at.%. As the total concentration of Ag in the base alloy is 3 at.%, about 2 at.% Ag is expected to be present as secondary Ag phase. Ag peaks were indeed observed in the XRD pattern of the as-rolled sample (see Fig. 1). According to the equilibrium phase diagram of the Cu-Ag system, the solubility limit of Ag in Cu is 4 at.% at 750 °C, therefore during the homogenization heat-treatment all Ag atoms were dissolved in the Cu matrix. The Ag precipitates observed in the as-rolled samples might form during quenching to RT and/or subsequent rolling process at LNT. Nevertheless, the Cu matrix with ~1 at.% solute Ag concentration after rolling is supersaturated since the equilibrium solubility limit of Ag in Cu is practically zero at RT. The microstructural parameters of the Cu matrix in the LNT rolled sample obtained by X-ray line profile analysis are presented in Table 1. The crystallite size in the as-rolled condition (~30 nm) is much smaller and the dislocation density is significantly higher (~48 × 10^{14} m^{-2}) than the values reported in pure Cu processed by different SPD methods [13-15]. This observation can be explained by the pinning effect of Ag on dislocations and grain boundaries formed during SPD. A TEM image obtained on RD-TD plane (RD: rolling direction, TD: transverse direction) of LNT rolled sample is shown in Fig. 2a. The grain size of the Cu matrix estimated from the TEM image is in the range of 100-200 nm. This value is much larger than the crystallite size obtained by XRD. This observation is in accordance with former studies and can be explained by the fact that the crystallite size usually corresponds to the subgrain size in severely deformed microstructures [16].

Table 1. The solute Ag concentration (c_{Ag}) and the parameters of the microstructure for the Cu matrix in the Cu – 3 at.% Ag alloy in the LNT rolled and LNT rolled + annealed conditions: $<x>_{area}$: area-weighted mean crystallite size, ρ: dislocation density, β: twin boundary probability.

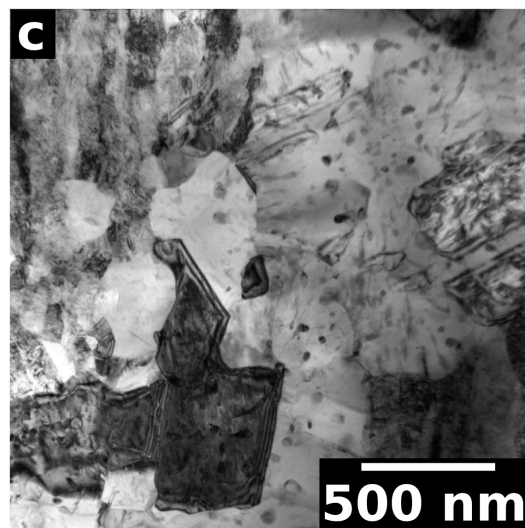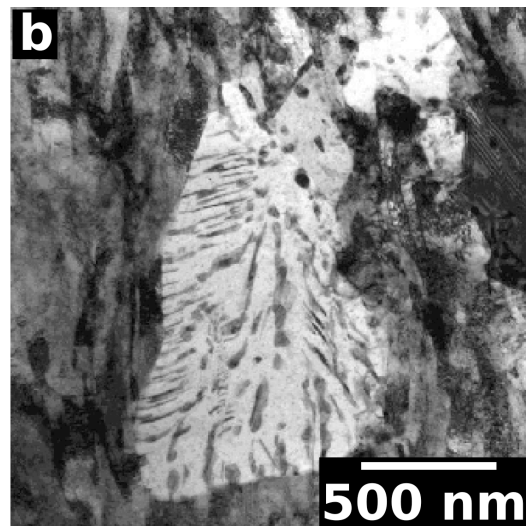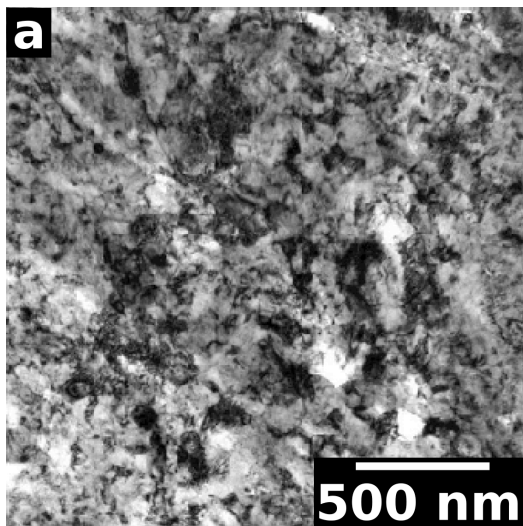| Sample	Region	c_{Ag} [at.%]	$<x>_{area}$ [nm]	ρ [10^{14} m^{-2}]	β [%]
LNT rolled		1.0 ± 0.1	30 ± 3	48 ± 5	0.5 ± 0.1
Annealed for 5 min	1	0.7 ± 0.1	25 ± 3	23 ± 4	0.2 ± 0.1
	2	2.6 ± 0.2	43 ± 5	25 ± 4	<0.05
Annealed for 10 min	1	0.3 ± 0.1	22 ± 3	5 ± 1	<0.05
	2	2.1 ± 0.2	45 ± 5	25 ± 3	0.1 ± 0.1
Annealed for 15 min	1	0.3 ± 0.1	23 ± 3	5 ± 1	<0.05
	2	2.3 ± 0.2	58 ± 6	22 ± 3	0.1 ± 0.1
Annealed for 20 min	1	0.3 ± 0.1	75 ± 8	2 ± 1	<0.05
	2	2.3 ± 0.3	49 ± 5	21 ± 2	0.2 ± 0.1

Figure 2. TEM images of the microstructure in the LNT rolled state (a), and after annealing for 10 (b) and 20 min (c) at 623 K.

Folowing annealing of the LNT rolled samples, each diffraction peak of the Cu matrix splits into two components. As an example, Fig. 3 shows reflection 220 for the sample annealed for 20 min. For comparison purpose, the same reflection for the LNT rolled specimen is also presented. The splitting of the peaks is believed to be caused by the development of an inhomogeneous solute atom distribution in the Cu matrix during annealing, resulting in a variation of the lattice parameter of the Cu matrix. Each line profile was evaluated by fitting it with the sum of two profile components having different Bragg-angles which correspond to two distinct regions of the matrix having different average lattice parameters. It should be noted that most probably the description of the distribution of the solute concentration by only two distinct solute contents is a simplification. Nevertheless, this procedure characterizes the inhomogeneity of the chemical composition of the matrix. The Ag solute concentrations in the two regions of the matrix have been determined from the lattice parameters of the two Cu phases obtained from the subprofile positions and listed in Table 1. The volumes with lower and higher Ag contents are referred to as Regions 1 and 2, respectively. The peaks of Regions 1 and 2 are at higher and lower diffraction angles, respectively. In Region 2 the solute Ag concentration considerably increased during annealing, which suggests partial dissolution of the Ag particles. The solute Ag content increased from ~1 at.% to 2.6 ± 0.2 at.% even after 5 min annealing and remained the same within the experimental error at least up to 20 min.
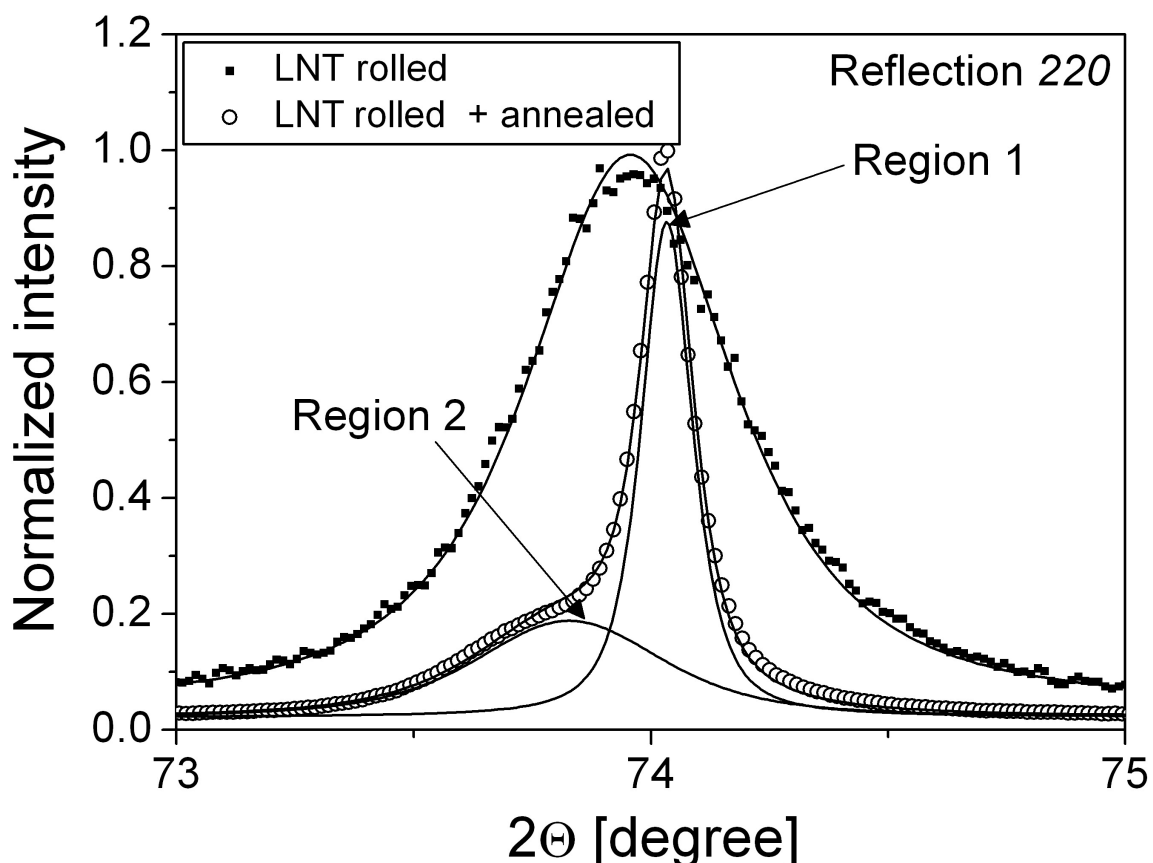

Figure 3. The CMWP fitting for 220 reflection of the Cu – 3 at.% Ag samples in LNT rolled state, and after annealing for 20 min at 623 K. The symbols and the solid lines represent the measured data and the fitted curves, respectively. The diffraction peak in the annealed condition is a sum of two reflections related to regions 1 and 2 having different average lattice parameters.

The microstructures in Regions 1 and 2 with different Ag contents obtained after annealing of the LNT rolled sample were investigated by X-ray line profile analysis. In the fitting of the experimental patterns, each theoretical line profile consisted of two peaks corresponding to the two regions. The microstructural parameters for Regions 1 and 2 of the Cu matrix were determined from the fitting and are listed in Table 1. The results reveal that in region 1 the crystallite size did not change considerably up to 15 min then increased by a factor of three for 20 min annealing. In this region, the dislocation density decreased only slightly after 5 min at 623 K, but it reduced by about one order of magnitude between 5 and 10 min. In region 2, the crystallite size increased slightly from 30 to 44 nm and the dislocation density decreased to about half during 5 min annealing and then both parameters remained unchanged within the experimental error at least up to 20 min. It can be concluded that in the volumes where the dissolution of the precipitates was negligible (Region 1), the solute Ag content remained low and the dislocation density decreased significantly due to recovery. However, the increased concentration of solute Ag atoms in Region 2 hindered the recovery, resulting in the retention of the high dislocation density. The separation of the microstructure into two regions with low and high defect densities is also confirmed by the TEM images presented in Figs. 2b and c for 10 and 20 min annealing times, respectively. The large grain in the middle of Fig. 2b contains numerous Ag particles while it does not exhibit considerable lattice distortions, while the surrounding fine-grained regions show distortion contrast. Most probably, the former and the latter volumes correspond to Regions 1 and 2, respectively. Similarly, a distorted UFG volume without Ag particles can be seen in the upper left corner of Fig. 2c, while the other regions do not show distortion contrast but they contain Ag precipitates.

4. Discussion

The decrease of the solute Ag content during annealing in Region 1 can be easily understood since the cryorolled alloy with the Ag concentration of ~1% is supersaturated at 623 K (the equilibrium solubility limit is 0.33%). It is noted that the solute Ag concentration in Region 1 is 0.3% for annealing times larger than 10 min which agrees with the equilibrium value of 0.33% (see Table 1). However, the partial dissolution of Ag precipitates in Region 2 is surprising at first sight. This observation is confirmed by the decrease of the relative integrated intensity of XRD peaks for Ag phase from about 8 to 5% due to annealing. This phenomenon could be caused by the large specific energy (energy per unit volume) for interfaces between Ag nanoparticles and the Cu matrix which yielded an enhanced equilibrium solubility limit of Ag in Cu. This solubility limit depends on the size of Ag dispersoids as expressed by the Gibbs–Thomson formula (also referred to as Ostwald–Freundlich equation) [17,18]:

$$c_d = c_\infty \, exp\left(\frac{2A\gamma V_m}{dRT}\right), \tag{1}$$

where d is the diameter of the spherical Ag precipitates, T is the temperature of annealing (623 K), c_∞ (0.33 at.%) and c_d are the equilibrium solute Ag concentrations in the Cu matrix with Ag precipitates having infinitely small curvature (large diameter) and diameter of d, respectively, γ is the interface energy between the Cu matrix and the Ag precipitates, R is the molar gas constant, V_m is the molar volume of Ag (10^{-5} m^3/mole) and A is a constant with the value of 2 or 3, depending on the assumptions made in the derivation of eq. (1). For instance, assuming incoherent interfaces between Ag and Cu with the specific energy of ~1.5 J/m^2 [19] and A=3, the Ag concentration at the temperature of annealing (623 K) is plotted as a function of the diameter of Ag particles in Fig. 4 (solid line). For precipitate sizes smaller than ~15 nm the value of c_d obtained from eq. (1) is higher than the average solute Ag concentration measured in the cryorolled sample (1 at.%). Therefore, the smaller Ag nanoparticles in the size distribution start to dissolve into the Cu matrix during annealing. The size of

these small Ag precipitates decreases while the solute Ag concentration in the surrounding Cu matrix increases. In Region 1, the decrease of Ag solute concentration could occur by the growth of the existing Ag particles. In this case, the size of Cu crystallites between the Ag particles should decrease which is in accordance with the results of X-ray line profile analysis (see Table 1). At the same time, in Region 2 the dissolution of Ag precipitates yielded an increment in Cu crystallite size. It should be noted that for the largest applied annealing time (20 min) the Cu crystallite size in Region 1 started to increase most probably due to a strong recovery and/or partial recrystallization.
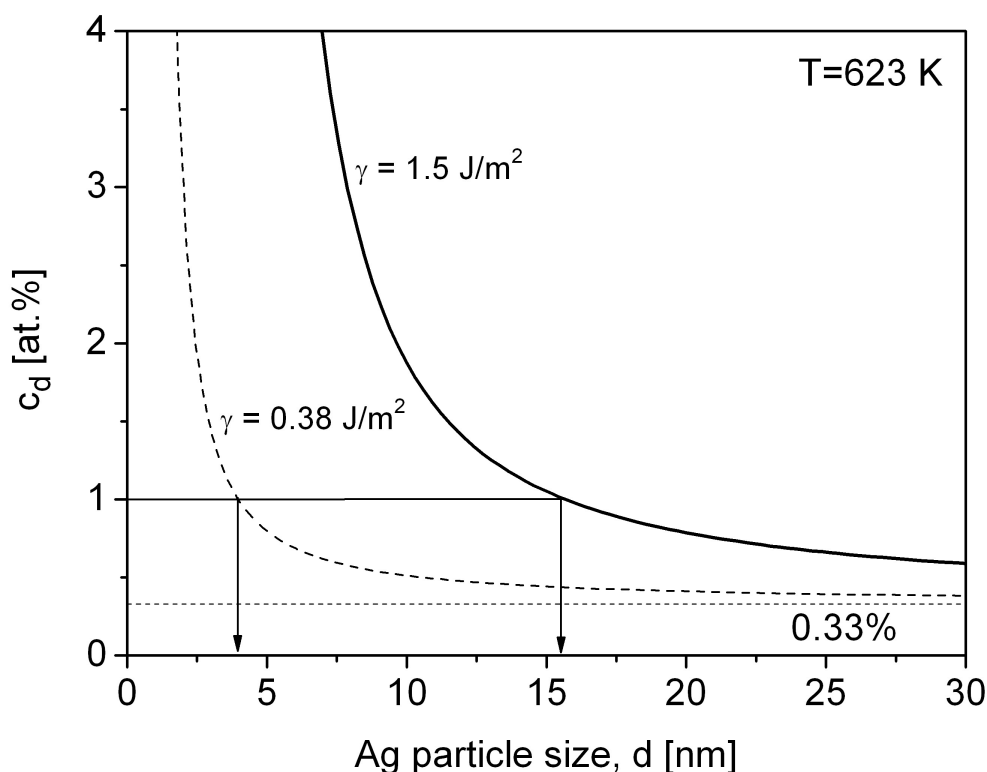

Figure 4. The equilibrium Ag solute concentration in the Cu matrix as a function of the size of Ag nanoparticles at 623 K for specific interface energies of 1.5 and 0.38 J/m^2.

It should be noted that the assumption for the incoherency of Ag/Cu interfaces might overestimate the interface energy value substituted into eq. (1). For instance, the energies of coherent 111/111 and 100/100 Ag/Cu interfaces are 0.23 and 0.53 J/m^2, respectively [20]. These values are much lower than that for incoherent interfaces (see above). Electron diffraction experiments carried out on the sample annealed for 20 min revealed that in Region 1 there is an epitaxial crystallographic orientation relationship between the Cu and Ag crystallites, as shown in the inset of Fig. 5. The areas with Moiré fringes correspond to the Ag particles grown epitaxially to the Cu crystallites. The Moiré pattern is caused by the difference between the interplanar spacings of (111) planes in Cu and Ag (the crystallographic direction $\left[12\bar{3} \right]$ is perpendicular to the image plane). The former and the latter spacings are $d_{Cu} = 0.2087$ and $d_{Ag} = 0.2359$ nm, respectively. According to Ref. [21] the spacing of the resulted translational Moiré fringes (d_M) can be obtained as:

$$d_M = \frac{d_{Ag} d_{Cu}}{d_{Ag} - d_{Cu}}. \tag{2}$$

Eq. (2) yields d_M = 1.81 nm which agrees with the experimentally determined value of 1.8 nm which confirms that the areas with Moiré fringes correspond to epitaxially grown Ag particles in the Cu matrix. The size of Ag precipitates in Fig. 5 is 10-30 nm. The lower specific energy of epitaxial interfaces results in a better stability of the nanosized Ag particles. Substituting the arithmetic average of the energies of 111/111 and 100/100 Ag/Cu interfaces (0.38 J/m^2) into eq. (1), indicates that only the Ag particles smaller than 4 nm will dissolve (see Fig. 4). Therefore, the volumes where the dissolution of Ag precipitates occurred during annealing (Region 2) are most probably the regions in which the Ag particles have very small size and/or large specific interface energy. Due to the spatially heterogeneous dissolution an inhomogeneous dislocation structure was also developed during annealing. In Region 1 the dislocation density strongly decreased while in region 2 the dislocation density remained relatively high. This heterogeneous microstructure yielded an improvement of the ductility while retaining the high strength as shown in our previous study [8]. In order to investigate the thermal stability of the high dislocation density in Region 2 studies with longer heat-treatments at 623 K will be carried out.
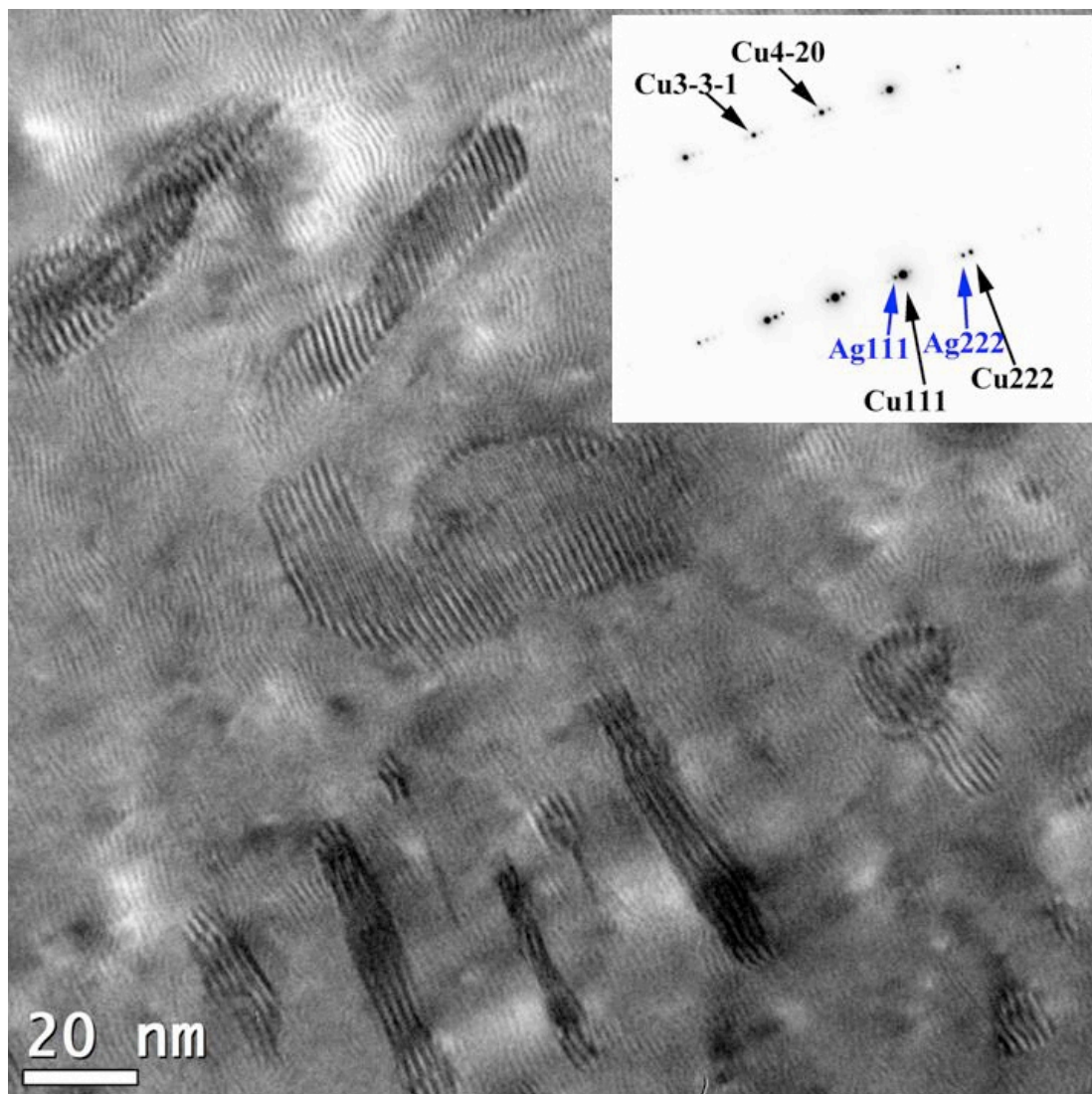
Figure 5. HRTEM image obtained on the cryorolled sample after annealing for 20 min. The selected area diffraction pattern is also shown in the inset. The areas with Moiré fringes correspond to epitaxially grown Cu and Ag crystallites.

5. Conclusions

Supersaturated Cu – 3 at.% Ag alloy was subjected to rolling at LNT and subsequent annealing at 623 K up to 20 min. In the annealed samples, an inhomogeneous solute atom distribution developed in the Cu matrix due to the dissolution of Ag nanoparticles in the regions where the Ag particles have very small size and/or large specific interface energy with the Cu matrix. In the volumes where the Ag solute content did not increase the dislocation density developed during cryorolling decreased by more than one order of magnitude after annealing for 20 min, while in the regions where the solute concentration increased the dislocation density in the Cu matrix reduced only to half of the value obtained after cryorolling. Therefore, the rolled and subsequently annealed samples exhibited heterogeneous microstructures where both the dislocation density and the solute concentration varied considerably.

References
[1] Valiev R Z, Langdon T G 2006 *Prog. Mater. Sci.* **51** 881
[2] Zhilyaev A P, Langdon T G 2008 *Prog. Mater. Sci.* **53** 893
[3] Gubicza J, Chinh N Q, Krállics Gy, Schiller I, Ungár T 2006 *Curr. Appl. Phys.* **6** 194
[4] Kuzel R, Janecek M, Matej Z, Cizek J, Dopita M, Srba O 2010 *Metall. Mater. Trans. A* **41** 1174
[5] Tsuji N, Ito Y, Saito Y, Minamino Y 2002 *Scripta Mater.* **47** 893
[6] Wang Y, Chen M, Zhou F, Ma E 2002 *Nature* **419** 912
[7] Shanmugasundaram T, Subramanya Sarma V, Murty B S, Heilmaier, M 2008 *Mater. Sci. Forum* **584-586** 97
[8] Sitarama Raju K, Subramanya Sarma V, Kauffmann A, Hegedűs Z, Gubicza J, Peterlechner M, Freudenberger J and Wilde G 2013 *Acta Mater.* **61** 228
[9] Nelson J, Riley J D 1945 *Proc. Phys. Soc. Lond.* **57** 160
[10] Ribárik G, Gubicza J, Ungár T 2004 *Mater. Sci. Eng. A* **387-389** 343
[11] Lábár J L 2005 *Ultramicroscopy* **103** 237
[12] Song J, Li H, Li J, Wang S, Zhou S 2002 *Appl. Optics* **41** 5413
[13] Zhao Y H, Liao X Z, Horita Z, Langdon T G, Zhu Y T 2008 *Mater. Sci. Eng. A* **493** 123
[14] Setman D, Schafler E, Korznikova E, Zehetbauer M J 2008 *Mater. Sci. Eng. A* **493** 116
[15] Gubicza J, Dobatkin S V, Khosravi E, Kuznetsov A A, Lábár J L 2011 *Mater. Sci. Eng. A* **528** 1828
[16] Gubicza J 2012 *Defect structure in nanomaterials* (Cambridge: Woodhead)
[17] Perez M 2005 *Scripta Mater.* **52** 709
[18] Kaptay G 2012 *J. Mater. Sci.* **47** 8320
[19] Delogu F J 2010 *Phys. Chem. C* **114** 19946
[20] Bacher P, Wynblatt P Foiles S M 1991 *Acta metall. mater.* **39** 2681
[21] Williams D B, Carter C B 2009 *Transmission Electron Microscopy* (New York: Springer)